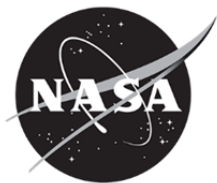NASA/TM–2014-218289

Investigating Delamination Migration in Composite Tape Laminates

James G. Ratcliffe
Langley Research Center, Hampton, Virginia

Nelson V. De Carvalho
National Institute of Aerospace, Hampton, Virginia

July 2014

NASA STI Program . . . in Profile

Since its founding, NASA has been dedicated to the advancement of aeronautics and space science. The NASA scientific and technical information (STI) program plays a key part in helping NASA maintain this important role.

The NASA STI program operates under the auspices of the Agency Chief Information Officer. It collects, organizes, provides for archiving, and disseminates NASA's STI. The NASA STI program provides access to the NASA Aeronautics and Space Database and its public interface, the NASA Technical Report Server, thus providing one of the largest collections of aeronautical and space science STI in the world. Results are published in both non-NASA channels and by NASA in the NASA STI Report Series, which includes the following report types:

- TECHNICAL PUBLICATION. Reports of completed research or a major significant phase of research that present the results of NASA Programs and include extensive data or theoretical analysis. Includes compilations of significant scientific and technical data and information deemed to be of continuing reference value. NASA counterpart of peer-reviewed formal professional papers, but having less stringent limitations on manuscript length and extent of graphic presentations.

- TECHNICAL MEMORANDUM. Scientific and technical findings that are preliminary or of specialized interest, e.g., quick release reports, working papers, and bibliographies that contain minimal annotation. Does not contain extensive analysis.

- CONTRACTOR REPORT. Scientific and technical findings by NASA-sponsored contractors and grantees.

- CONFERENCE PUBLICATION. Collected papers from scientific and technical conferences, symposia, seminars, or other meetings sponsored or co-sponsored by NASA.

- SPECIAL PUBLICATION. Scientific, technical, or historical information from NASA programs, projects, and missions, often concerned with subjects having substantial public interest.

- TECHNICAL TRANSLATION. English-language translations of foreign scientific and technical material pertinent to NASA's mission.

Specialized services also include organizing and publishing research results, distributing specialized research announcements and feeds, providing information desk and personal search support, and enabling data exchange services.

For more information about the NASA STI program, see the following:

- Access the NASA STI program home page at *http://www.sti.nasa.gov*

- E-mail your question to help@sti.nasa.gov

- Fax your question to the NASA STI Information Desk at 443-757-5803

- Phone the NASA STI Information Desk at 443-757-5802

- Write to:
  STI Information Desk
  NASA Center for AeroSpace Information
  7115 Standard Drive
  Hanover, MD 21076-1320

NASA/TM–2014-218289

Investigating Delamination Migration in Composite Tape Laminates

James G. Ratcliffe
Langley Research Center, Hampton, Virginia

Nelson V. De Carvalho
National Institute of Aerospace, Hampton, Virginia

Abstract

A modification to a recently developed test specimen designed to investigate migration of a delamination between neighboring ply interfaces in tape laminates is presented. The specimen is a cross-ply laminated beam consisting of 40 plies with a polytetrafluoroethylene insert spanning part way along its length. The insert is located between a lower 0-degree ply (specimen length direction) and a stack of four 90-degree plies (specimen width direction). The modification involved a stacking sequence that promotes stable delamination growth prior to migration, and included a relocation of the insert from the specimen midplane to the interface between plies 14 and 15. Specimens were clamped at both ends onto a rigid baseplate and loaded on their upper surface via a piano hinge assembly, resulting in a predominantly flexural loading condition. Tests were conducted with the load-application point positioned at various locations along a specimen's span. This position affected the sequence of damage events during a test. Delamination growth occurred prior to migration in specimens loaded at a location near to and ahead of the insert front. Conversely, delamination migration occurred first in specimens loaded at a position further behind the insert front. In the former cases, variation of the load-application location was found to affect the distance relative to this point at which migration initiated. Migration initiated in each specimen by a gradual transition of the delamination at the 0/90 interface into the 90-degree ply stack. In contrast, transition into the new 90/0 interface was sudden. A delamination resistance mechanism was observed that arose from delamination actually delving slightly into the lower 0-degree ply prior to migration. This implies that such an effect may be present during delamination at a non-unidirectional ply interface in any laminates subjected to flexural loading.

Introduction

Delamination is a failure mode commonly associated with composite tape laminates, and has thus received considerable attention focused on delamination as an individual mode of failure. For instance, considerable effort has been paid toward characterizing individual delamination, driven under mode-I, mode-II, mode-III and a mixture of these loading conditions [1-4]. Meanwhile, analysis methods have been developed that simulate delamination onset and growth along one ply interface without the possibility for migration of that delamination to another interface [5, 6]. While such analyses are adequate in many situations, delamination growth in laminates commonly involves migration between different ply interfaces [7-10]. Methods are being developed within the finite element analysis framework that enable simulation of such migration events [11, 12]. Experimental work has also focused on investigating delamination migration in laminates and utilized tests that involve multiple migration events [9, 13]. More recently, a test method was developed that was designed to characterize delamination migration and provide benchmarking data for validation of analyses for simulating migration [14]. This test specimen, depicted in Fig. 1, is a cross-ply laminate with a mid-plane insert spanning part way along the specimen length. The specimen is loaded to first cause onset of delamination growth from the insert front followed by migration of this delamination to another ply interface within the specimen. Overall, the delamination growth and migration events occur uniformly across the specimen width and thus the test yields data against which 2-dimensional analyses could be validated. One issue with the test is that

delamination growth onset and migration tend to be unstable events, which makes simulating the test for validation purposes more cumbersome. The purpose of the work described here was to modify the stacking sequence of this delamination migration test specimen in order to promote stable delamination growth and migration. To this end, a series of analyses were conducted in order to determine an appropriate specimen stacking sequence. Specimens were manufactured, tested and examined for documentation of delamination migration.

Delamination Migration Tests

Specimen Configuration

The delamination migration test configuration is illustrated in Fig. 1 and is identical to that introduced recently [14]. The specimen possesses three main features that permit the controlled observation of delamination growth followed by a single migration event to another ply interface. First, the specimen is a cross-ply beam that yields uniform delamination growth and migration across the specimen width, such that observations from the specimen edges provide a good indication of fracture taking place through the specimen width. Second, the specimen contains a PTFE insert (acting as an artificial delamination) at an interface between a 0-degree ply (specimen span direction) and a stack of four 90-degree plies (specimen width direction). The 0-degree ply acts to confine the delamination to this 0/90 interface by preventing the delamination from migrating through this ply. The 90-degree ply stack provides a path for the delamination to kink in to, leading to eventual migration. Third, the specimen can be loaded in a manner to cause delamination growth from the PTFE insert that eventually migrates to another ply interface. This sequence of fracture events is made possible by the way in which specimen loading affects shear stresses acting across the delamination front, in a manner described previously by Greenhalgh et al [15]. This process is illustrated in Fig. 2. In the case of the loading configuration illustrated in Fig. 2a (delamination front to the left of the load-application point), the shear stress acting across the PTFE insert front promotes kinking of the delamination towards the baseplate side of the specimen. However, the 0-degree ply below the PTFE insert prevents this from occurring, and instead, delamination grows along the 0/90 ply interface. The delamination continues to propagate along the 0/90 interface and grows past the load-application point (Fig. 2b), eventually leading to a reversal of the sign of the shear stress acting across the delamination front. The shear stress now promotes kinking of the delamination into the 90-degree ply stack towards the loaded side of the specimen, leading to complete migration of the delamination. More specific details regarding this migration process as it pertains to the current specimen can be found in [14].

Materials and Specimen Stacking Sequence

The composite material selected for this investigation was a IM7/8552 carbon/epoxy tape pre-preg manufactured by Hexcel [16]. In the current work, the specimen stacking sequence utilized for the original migration specimens [14] was modified to promote stable delamination growth onset and propagation. Hence, migration should be relatively more discernable from the specimen response, unlike migration in the original specimens, which took place during an unstable event where delamination growth also occurred [14].

Alternative stacking sequences for the migration specimen were evaluated by conducting 2-dimensional finite element analyses of the specimen. The dimensions of the specimen

2

considered in the analyses are given in Fig 1. The analyses were almost identical to those described in Ref. 14 (details of the finite element mesh, loading and boundary conditions are given in [14]). In the original migration specimens, the pre-implanted PTFE insert was located at the specimen mid-plane. Different positions within the specimen were considered in the current work on the hypothesis that shifting the insert away from the specimen mid plane may help to stabilize delamination growth. Four different load-application point positions (dimension, L, in Fig. 1) were considered. These locations corresponded to those examined experimentally in previous migration tests [14]. The four positions were as follows: $L=a_0$, $1.1a_0$, $1.2a_0$ and $1.3a_0$, where the dimension, a_0, is the length of the PTFE insert as illustrated in Fig. 1. A set of different delamination lengths (beginning with a length of a_0) were considered for each loading position in order to manually represent delamination growth. The same prescribed displacement (z=1mm, Fig.1) was used in each analysis in order to emulate the displacement controlled loading under which the actual migration tests were conducted.

Upon completion of each analysis, the virtual crack closure technique (VCCT) [5] was utilized to compute the energy release rate G_T (and its components G_I and G_{II}) for a set of fixed delamination lengths. Following [17], the critical load and displacement for each delamination length was obtained by linearly scaling the prescribed displacements and load:

$$P_{crit} = P\sqrt{\frac{G_c}{G_T}}, \ \delta_{crit} = \delta\sqrt{\frac{G_c}{G_T}}$$ (1)

where critical energy release rate, Gc, was assumed to be given by a mixed mode exponential law [17]. The resultant critical load-displacement curve was then used to assess the stability of each candidate layup, under displacement-control conditions. Additionally, for each stacking sequence, the specimen bending-twist coupling and the specimen's ability to withstand the expected load levels were also assessed.

The final stacking sequence chosen for the current specimens based on results from the above finite element analyses is shown in Fig. 3a. For comparison, the original stacking sequence [14] is shown in Fig. 3b. The overall number of plies in the current stacking sequence is the same as that in the original specimens. The main difference between the two stacking sequences is the location of the pre-implanted PFTE insert, which has been moved from the mid-plane down towards the lower portion of the specimen. The plies bounding the delamination (a lower 0-degree ply and an upper stack of four 90-degree plies) are the same as in the original specimen. The delamination is now located between ply 14 and 15 of the 44-ply laminate (ply #1 beginning from the bottom of the specimen as depicted in Fig. 3a).

An example result from a finite element analysis of a specimen with the new stacking sequence and loading position, $L=1.1a_0$, is shown in Fig. 4, which is a plot of applied load, P versus load-point displacement, δ. The plot compares the critical load-displacement responses of a specimen with the original (OR) [14] and with the redesigned stacking sequence (S0). For the case considered in Fig. 4, the original stacking sequence shows unstable delamination growth under displacement-controlled conditions. This finding is in agreement with delamination growth observed in actual specimens [14]. Conversely, the redesigned layup shows stable delamination under displacement-controlled loading, as intended. Complementary analysis also showed that the extension-bending coupling of the redesigned layup was of the same order of magnitude as of the original layup [14], and that it was capable of withstanding the expected load range, confirming its suitability for testing.

Tests performed on actual migration specimens with the stacking sequence selected as a result of the current study confirmed that delamination growth in these specimens is mostly stable. Details of these tests are presented next.

Delamination Migration Tests

Specimens were loaded with 6 nominal loading positions: $L=0.5a_0$, $0.8a_0$, a_0, $1.1a_0$, $1.2a_0$, and $1.3a_0$ (where $a_0=48$mm). Four repeat specimens of each load position were tested, resulting in a total of 24 specimens.

The migration tests were conducted using a servo-hydraulic test machine equipped with a 22,250N load cell whose range was scaled to 2225N. Specimens were secured into the loading fixture pictured in Fig. 5. Specimens were clamped at both ends and loaded via a piano hinge bonded to the upper surface of the specimen. Precise details of the test fixture can be found in [14]. After proper alignment was established with the specimen length perpendicular to the hinge axis, specimens were loaded under displacement control at a rate of 0.127mm/min in the direction indicated in Fig. 1. Specimens were unloaded at the same loading rate. Applied load and crosshead displacement (referred to as displacement in the remainder of the paper) were recorded throughout each test. Delamination growth and migration was recorded by viewing both sides of each specimen using a pair of cameras equipped with macro lenses. Images of the delamination and migration events were recorded as they occurred during a test. The cameras were synchronized with the force and displacement output collected by the data acquisition system, enabling documentation of the exact force and displacement associated with each image.

Post-Test Inspection

The delamination and migration paths as viewed from both edges were inspected using an optical microscope at a 40-80X-magnification level. A selection of specimens tested with each loading position was inspected using X-ray computed tomography in order to gain an understanding of the fracture mechanisms within the body of the specimens. Specimens were also sectioned along the z-y plane (see coordinate system in Fig. 1) and examined under an optical microscope at a 40X-160X-magnification level. In addition, specimens were split along the existing delamination plane in order to confirm the PTFE insert front location.

Results/Discussion

Specimen Response

The applied load versus load-point displacement of a single specimen tested at each of the six loading points is shown in Fig. 6. The four repeat specimens of each load position exhibited consistent responses and thus a single case is shown in Fig. 6 to aid the comparison between the six cases. All specimens exhibited linear loading and unloading responses. In all cases, except for a loading position, L, equal to $0.5a_0$, delamination growth took place prior to migration. Generally, the distance from the load application point at which migration initiated, Dk, (see Figs. 7-12) decreased with increasing load position. The distance ranged from approximately 13mm at $L=1.3a_0$, to 16mm at $L=0.85a_0$. These findings are generally consistent with previous tests [14] and are discussed in more detail in the next section. Delamination growth onset was moderately unstable in all cases and was proceeded by mostly stable

propagation until migration occurred, which was usually signified by a sudden load drop as indicated in Fig. 6. The specimens with a loading position, $L=0.5a_0$ exhibited delamination migration immediately from the PFTE film insert. This was expected given that the shear stresses acting in the vicinity of the insert front tend to favor kinking of the delamination into the upper 90-degree ply stack. Migration initiated in these specimens at around 73% of the peak load. This was indicated by a very slight drop in load (at approximately 80N in the example shown in Fig. 6). Migration was eventually completed upon further loading, indicated by a small load drop (at approximately 110N in the example shown in Fig. 6). Sample load-displacement responses from each of the six load positions are given in Figs. 7-12 and include specimen edge views at key stages of each test (note, that the same force-displacement data shown in Fig. 6 are shown in Figs. 7-12).

A comparison of the load-displacement responses of the current specimens with responses of the original specimens [14] for load positions, $L=a_0$, $1.1a_0$ and $L=1.2a_0$, $1.3a_0$ is presented in Figs. 13 and 14, respectively. The comparison shows that delamination growth in the current specimens is relatively more stable than in the original specimens rendering migration generally more discernable from the response of the current specimens. For instance, in Fig. 13, the sudden load drop of the original specimen [14] (loading position, $L=1.1a_0$) involved around 15mm of delamination and migration. By contrast, delamination propagation (around 14mm of growth) in the current specimen with the same load position took place in a relatively stable manner prior to migration. Thus, specimens with the alternative stacking sequence satisfy the first objective of the current work, which was to encourage stable delamination propagation. However, the final unstable event that was typically exhibited by all specimens (that exhibited delamination prior to migration) involved around 1-3mm of delamination growth in addition to the migration event. Therefore the actual moment of migration is not exactly discernable from the specimen load-displacement response except for specimens that migrated immediately from the PTFE film insert. In specimens where delamination propagation occurred prior to migration (all load positions except $L=0.5a_0$), specimen loading tends to increase (after initial delamination growth onset) as delamination propagation takes place. This effect was not anticipated from the finite element analyses conducted to evaluate candidate stacking sequences. For instance, with the new stacking sequence and load position, $L=1.1a_0$, the applied load was predicted to decrease as delamination propagation takes place prior to migration (response of S0 in Fig. 4). Although initial delamination growth is accompanied by a gradual reduction in load during actual tests with this load position ($L=1.1a_0$ in Figs. 6 and 13), the load eventually begins to increase upon further delamination until the instance of migration. In this example, the load at delamination growth onset is approximately 210N and the load increases to 260N at the point of migration after 20mm of delamination propagation. A similar behavior was observed in all other specimens (except for specimens with the load position, $L=0.5a_0$).

In the analysis, *Gc* was computed as a function of the mixed mode ratio, using an exponential law [17]. *Gc* for delamination onset and growth were assumed to be the same. Therefore, the increase in load observed experimentally, and not predicted in the analysis, suggests an increase in *Gc* with delamination growth.

The investigation of this apparent increase in resistance with delamination growth is presented in later in the section entitled, Nature of Delamination Growth and Migration.

Effect of Load Position on Migration

The plot in Fig. 15 shows the distance from the load-application point at which delamination migration onset was observed (Δk) as a function of normalized load position, L/a_0. Each data point represents an average of four repeat tests. Although the scatter in these data between repeat specimens at a given load position is moderately high (standard deviations ranged between 1 and 3mm), the overall data tend to show that migration onset occurs closer to the load-application point as the load position increases. Corresponding data from the previous

migration tests [14] are included in Fig. 15 for comparison and exhibit a similar trend to the current data (at least for L/ a_0>1). A previous explanation for this trend was that the load position affects the mixed-mode loading condition driving delamination growth, ultimately altering the location at which migration takes place. Migration, however, took place slightly further from the load-application point in the current specimens, which is most likely due to the differing stacking sequence of the current specimens versus those tested previously [14].

A plot of kink angle, Ω, (see Fig. 2b) as a function of load position is also included in Fig. 15. Each data point represents an average from four repeat specimens at each load position. Corresponding data from the previous migration tests [14] are also included in the figure and show that kink angle in the current specimens is similar to that in previous specimens for a given load position. Kink angles in the current specimens generally reduced with load position, decreasing from 72 degrees at L≈$0.5a_0$ to 49 degrees at L=$1.3a_0$. Scatter in the current kink angle data was moderate with a maximum standard deviation of 11 degrees in the data corresponding to the load position, L=$1.3a_0$.

Nature of Delamination Growth and Migration

As discussed at the beginning of this section, a mechanism was observed that appears to resist delamination growth in the current specimens. This is manifested in a general increase in applied load as delamination occurs (as shown in Fig. 6). This mechanism was unexpected on the basis of the design analysis results, which predicted a general decrease in applied load with continuing delamination growth. In order to understand this resistance phenomenon, specimen delamination surfaces were examined using X-ray computed tomography. Following these X-ray inspections, specimens were sectioned and polished in order to reveal the location of delamination and migration with respect to the specimen plies local to these features.

Images of the upper delamination surface of a specimen from each of the six load positions, taken using X-ray computed tomography, are presented in Fig. 16 (the upper surface being that indicated in Fig. 3). The dark, horizontal bands that appear near to the bottom of each image correspond to the crack that kinked through the upper 90-degree ply stack resulting in migration.

The specimen with a load position, L=$0.5a_0$, exhibited migration immediately from the PTFE film insert. In all other cases a certain amount of delamination growth took place prior to the final migration event. The delamination surface in all these cases exhibits two common features. First, imprints of 0-degree fibers are apparent on the delamination surface and tend to transition into finger-like patterns up to the kinked crack region. Second, horizontal lines appear along the delamination surface part way towards the migration region. X-ray inspection confirmed that these lines are in fact cracks that kinked part or all the way through the upper stack of four 90-degree plies.

The imprints of the 0-degree fibers indicate that delamination growth partly dives under the surface of the bounding 0-degree ply during initial stages of delamination growth (typically before it has reached the load-application point). Specimens tested with each load position were also sectioned and the exposed surfaces polished in order to further explore where delamination took place prior to migration. Of the specimens that exhibited delamination prior to migration, the overall features were very similar. Images of polished sections of a specimen with a load position, L=$1.1a_0$, are presented in Fig. 17 and are from the same specimen of which an X-ray image is presented in Fig. 16. First, one of the specimen edges was polished and three images (labeled 1-3 in Fig. 17) were taken along the path of delamination growth beginning from the PTFE film insert-front region and ending at the migration (this edge corresponds to the left-hand side of the X-ray image of this specimen's delamination surface in Fig. 16). The images indicate that delamination growth from the insert front took place near to the 0/90 ply interface, which transitioned into the lower 0-degree ply upon further growth up to the moment of migration. The X-ray imaging also indicated that the extent with which delamination took place within the 0-degree ply varied along specimen width, therefore specimens were sectioned at the

locations shown in Fig. 17 (labeled Section AA and Section BB) in order to help further establish the location of delamination growth. Three images were taken at each section, the first (left-hand side) corresponding to the edge shown in images 1-3, the second (middle) corresponding to the specimen mid-width, and the third image (right-hand side) corresponding to the other edge of the specimen. The images generally confirm what was suspected from the previous observations: that delamination tends to remain near the 0/90 ply interface at the beginning of delamination growth, eventually transitioning just into the 0-degree ply (with the extent of this transition varying across the width). This delving of the delamination into the 0-degree ply causes some fibers to bridge the delamination, and therefore causes additional resistance to the delamination growth. This mechanism, referred to herein as ply delving, is thought to be an analogue to fiber bridging observed in characterization specimens such as the double cantilever beam specimen [18, 19]. This ply delving is thought to occur because of misalignment of fibers in the bounding 0-degree ply, which create paths for the delamination to propagate into the ply during the initial stages of growth when local shear stresses tend to kink the delamination towards this ply (see Fig. 2a). Furthermore, evidence of this ply delving near the mid-width region of the specimens (middle image of Section BB in Fig. 17) also implies that this is not simply an artifact of free-edge effects in the specimens.

After a certain amount of delamination growth (note, always after the delamination has propagated past the load application point), the shear stress changes sign, promoting kinking of the delamination up into the 90-degree ply stack. Notably, the kinked cracks that are evident prior to final delamination migration, Fig. 16, do not extend across the entire specimen width. As noted previously, the extent of ply delving into the bounding 0-degree ply varies across the width of the present specimens. In places where a lesser amount of delving has taken place, the delamination local to these regions begins kinking into the 90-degree ply stack (resulting in the horizontal lines in Fig. 16). However, more ply delving is evident in other positions across the specimen width, which helps to prevent kinking even when the local stress state makes this feasible. At this stage of delamination growth, the local shear stresses, which would now tend to kink the delamination through the 90-degree ply stack, are prevented from doing so by the bridging fibers that resulted from the ply delving. This is thought to essentially delay the moment at which migration occurs, which will do so once the propagating delamination is able to meander through the 0-degree ply up into the 90-degree ply stack. This mechanism is thought to be the reason for the finger-like patterns up to the region of migration evident in the X-ray images in Fig. 16.

Beyond confirming the nature of delamination growth in the present specimens, these findings offer possibly more general insight into the nature of delamination (driven by flexural loading such as that during a low-velocity impact event) in a laminate growing at a non-unidirectional ply interface. First, the current findings suggest that delamination growth will generally follow the fiber direction of the ply whose fibers can largely oppose the tendency of the delamination to otherwise kink through the ply (resulting in would-be migration). Second, once this so-called bounding ply facilitates delamination growth, inherent misalignment of fibers in this ply may result in the resistance effect resulting from the ply delving mechanism observed in the present specimens. A possible implication of these considerations is that some form of delamination resistance effect may often be present during delamination created under flexural loading at a multi-unidirectional ply interface. If this implication turns out to be true and is a significant effect, it should be included during simulations of delamination at non-unidirectional ply interfaces. This situation raises the question of how to characterize such a resistance effect for inclusion in an analysis. Of course, this effect may well be exclusive to the present specimens owing to the almost purely flexural load application and the unconventional stacking sequence utilized. However, this is yet to be confirmed and may serve as a useful focal point for a future study.

Concluding Remarks

A stacking sequence was identified that promotes stable delamination growth onset and migration in the delamination migration test specimen. Specimen responses were documented and the nature of delamination growth and migration was investigated. Generally, the position of the load-application point had a mild effect on the location along the length of a specimen in which migration took place. Closer examination of delamination prior to migration via X-ray computed tomography and optical inspection revealed that delamination tends to delve into the surface of the bounding 0-degree ply until the point of migration. Further examination suggested that this ply delving phenomenon was likely responsible for the delamination resistance effect observed in all specimens that exhibited delamination prior to the migration event. A possible implication of these observations is that some form of delamination resistance effect may often be present during delamination at a non-unidirectional ply interface in a laminate subjected to flexural loading. Hence, it may be necessary to include this resistance effect during simulations of delamination at non-unidirectional ply interfaces. Further study is required to determine how to best characterize such a resistance effect for inclusion in an analysis.

References

[1]   A.J. Russell "*Factors Affecting the Opening Mode Delamination of Graphite Epoxy Laminates*," Defense Research Establishment Pacific, DREP Materials Report 82-Q, 1982.

[2]   A.J, Russell "*On Measurement of Mode II Interlaminar Fracture Energies*," Defense Research Establishment Pacific (DREP), Victoria, British Columbia, Canada, Materials Report 82-0, December 1982.

[3]   J.R. Reeder and J.H. Crews "*Redesign of the Mixed-Mode Bending Delamination Test to Reduce Nonlinear Effects*," Journal of Composites Technology and Research, Vol. 14, pp 12-19, 1992.

[4]   S. Lee "*An Edge Crack Torsion Method for Mode III Delamination Fracture Testing,*" Journal of Composites Technology and Research, Vol. 15, pp 193-201, 1993.

[5]   E.F. Rybicki and M.F. Kanninen "*A Finite Element Calculation of Stress Intensity Factors by a Modified Crack-Closure Integral*," Engineering Fracture Mechanics, Vol. 9, pp 931-938, 1977.

[6]   P.P. Camanho, C.G. Davila and D.R. Ambur "*Numerical Simulation of Delamination Growth in Composite Materials*," NASA Technical Publication, NASA-TP-211041, 2001.

[7]   D. Hull and Y.B. Shi "*Damage Mechanisms Characterization in Composite Damage Tolerance Investigations*," Composite Structures, Vol. 23, No. 2, pp 299-120, 1993.

[8]   W.J. Cantwell and J. Morton. "*The Impact Resistance of Composite Materials — A Review*," Composites, Vol. 22, No. 5, pp 347–362, 1991.

[9]   R. Krueger, M.K. Cvitkovich, T.K. O'Brien and P.J. Minguet. "*Testing and Analysis of Composite Skin/Stringer Debonding under Multi-Axial Loading*," Journal of Composite Materials, Vol. 34, No. 15, pp 1263-1300, 2000.

[10] G.S. Owsley "*The Effect of Z-Fibre Reinforcement on Fatigue Properties of Stiffened Composite Panels*," Presented at the 15th Technical Conference of the American Society for Composites, Texas, September 25-27, 2000.

[11] T. Belytschko, R. Gracie1, and G. Ventura "*A Review of Extended/Generalized Finite Element Methods for Material Modeling*," Modelling and Simulation in Materials Science and Engineering, Vol. 17, No. 4, pp 1-24, 2009.

[12] D.L. Yang and B. Cox "*An Augmented Finite Element Method for Modeling Arbitrary Discontinuities in Composite Materials*," International Journal of Fracture, Vol. 156, No. 1, pp 53-73, 2009.

[13] C. Canturri, E.S. Greenhalgh, S.T. Pinho and J. Ankersen. "*Delamination Growth Directionality and the Subsequent Migration Processes – The Key to Damage Tolerant Design*," Presented at the 15th European Conference on Composite Materials, Venice, Italy, 24-28 June, 2012.

[14] J. Ratcliffe, M. Czabaj and T.K. O'Brien "*Characterizing Delamination Migration in Carbon/Epoxy Tape Laminates*," NASA Technical Memorandum, NASA-TM-2013-218028, August, 2013.

[15] Greenhalgh, E.S., C. Rogers, and P. Robinson. "Fractographic Observations on Delamination Growth and the Subsequent Migration Through the Laminate," Composites Science and Technology, Vol. 69, pp.2345-2351, 2009.

[16] Hexcel Corporation. "HexPly[®] 8552 Product Data Sheet," *http://hexcel.com*, 2007.

[17] R. Krueger "*Development and application of benchmark examples for mixed –mode I/II quasi-static delamination propagation predictions,*" NASA/CR-2012-217562, 2012.

[18] "ASTM D 5528-13, *Standard Test Method for Mode I Interlaminar Fracture Toughness of Unidirectional Fiber-Reinforced Polymer Matrix Composites*," in Annual Book of ASTM Standards. Vol. 15.03, American Society for Testing and Materials, 2014.

[19] W.S. Johnson and P.D. Mangalgari. "*Investigation of Fiber Bridging in Double Cantilever Beam Specimens*," Journal of Composite Technology and Research, Vol 9, pp. 10–13, 1987.
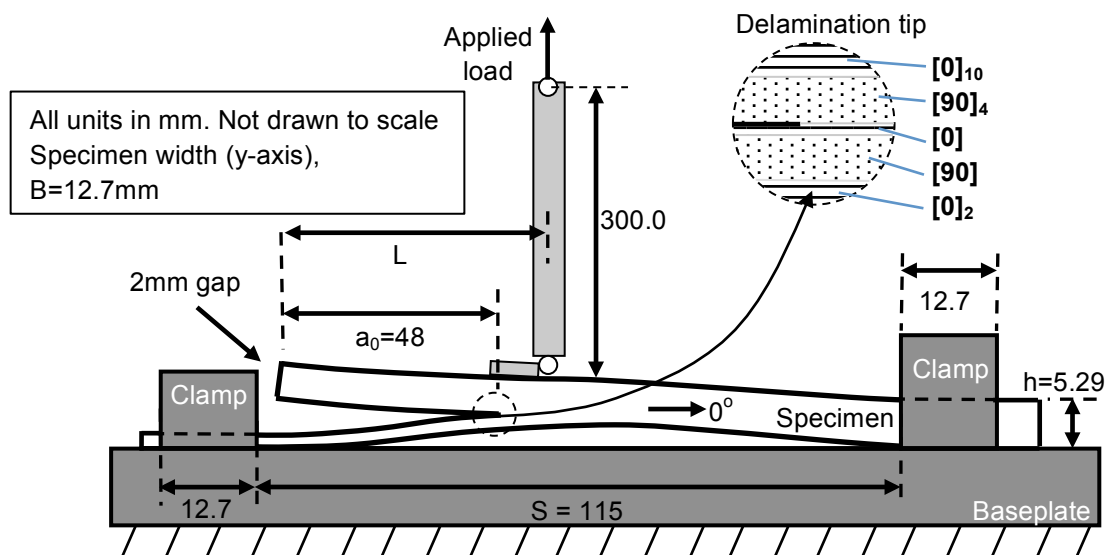
Fig. 1. Schematic of delamination migration test configuration.
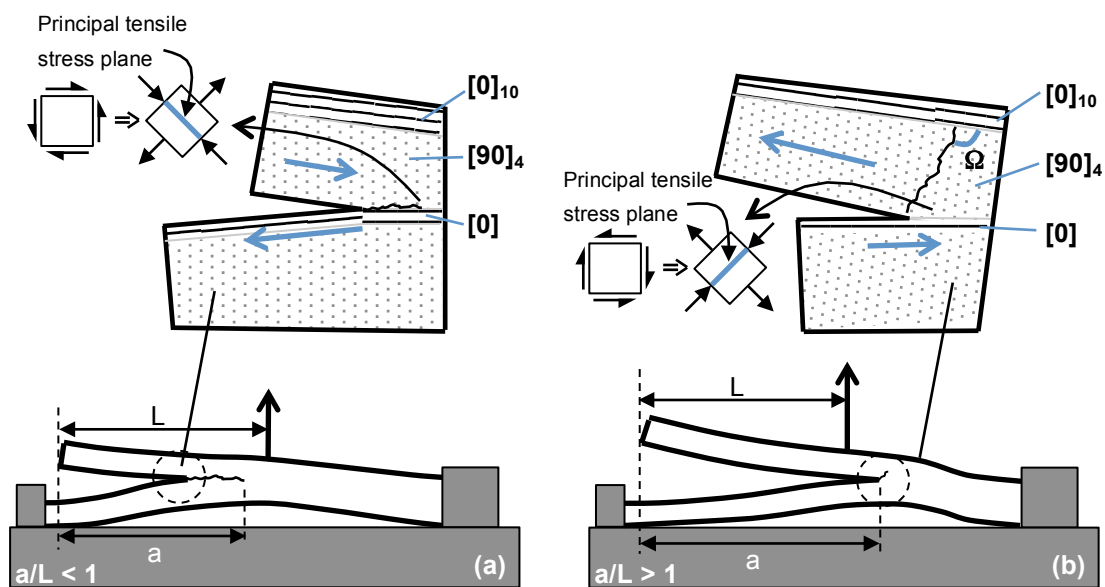
Fig. 2. Shear stresses acting across the delamination front at different stages of growth.

New stacking sequence and PTFE insert location:
$[0_4/90_{12}/0_{10}/90_4/$ **T**$/0/90/0_2/90_6/0_2/90/0]$

Upper delamination surface

(a)
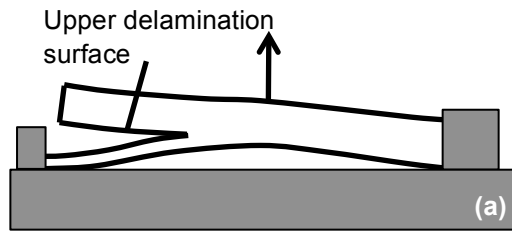
Original stacking sequence and PTFE insert location:
$[90_4/0_3/(90/0)_{2s}/0_3/90_4/$**T**$/0/90_4/0/0/(90/0)_{2s}/0/0/90_3/0/90]$

(b)
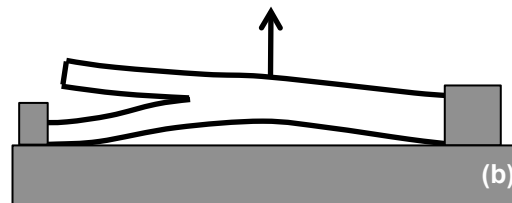
Notes:
Sequence of plies: Left to right corresponds to upper to lower surfaces of the specimen.
PTFE insert location indicated by letter, **T**.

Fig. 3. New versus original stacking sequences.

L=1.1a U

a

P [N]

unstable region

- - ◆ - - OR
——+—— S0

δ [mm]
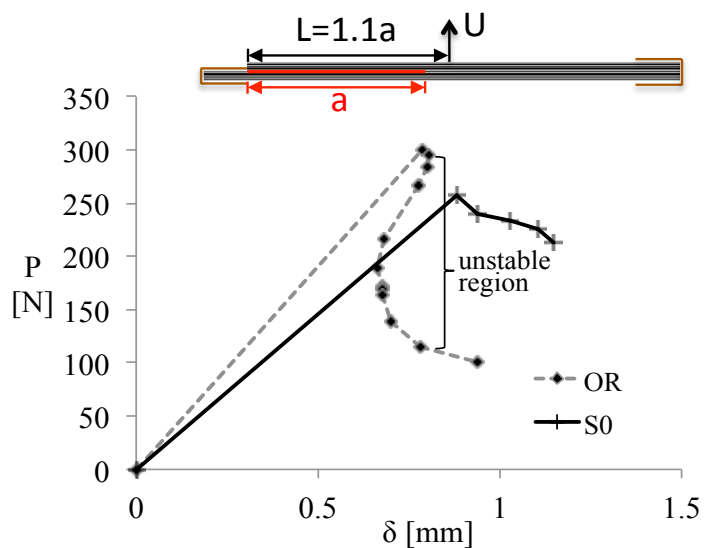
Fig. 4. Comparison between the critical load-displacement response of the original layup (OR) and of the redesigned layup (S0).
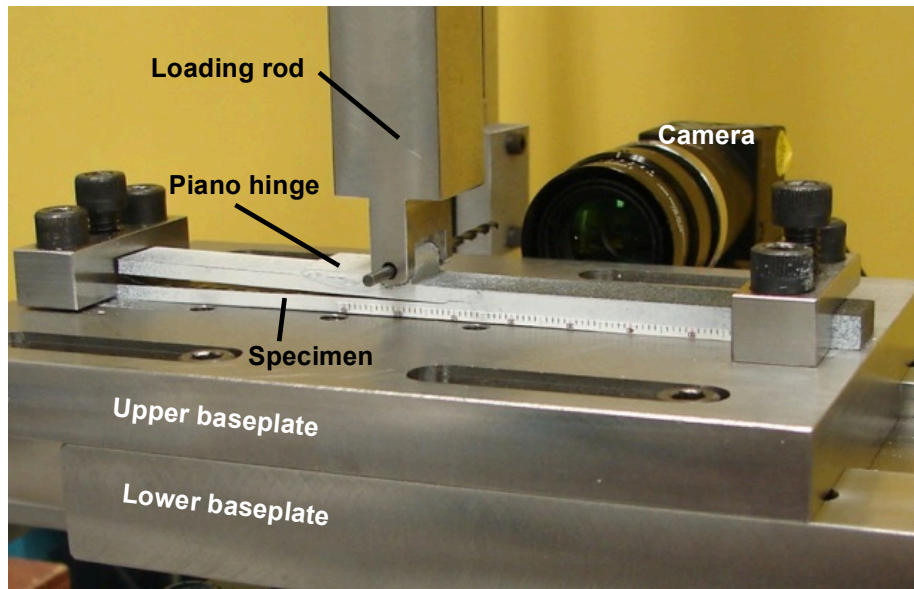
Fig. 5. Test fixture with loaded specimen.
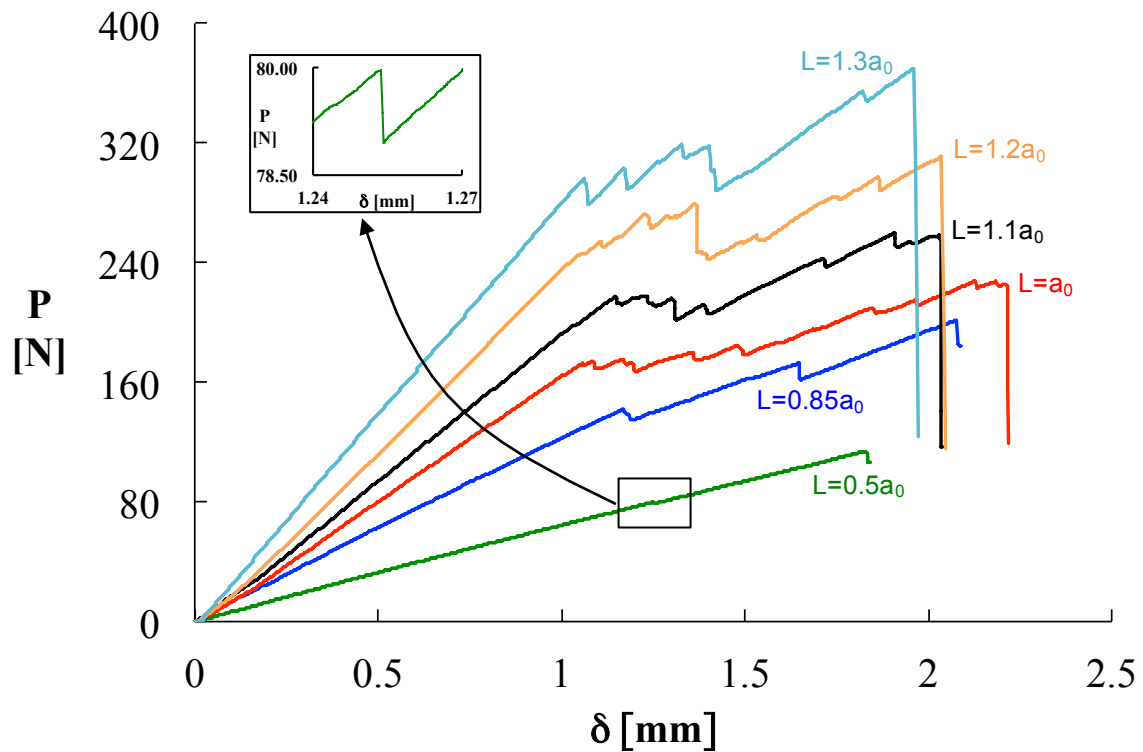
Fig. 6. Load displacement responses of migration specimens.
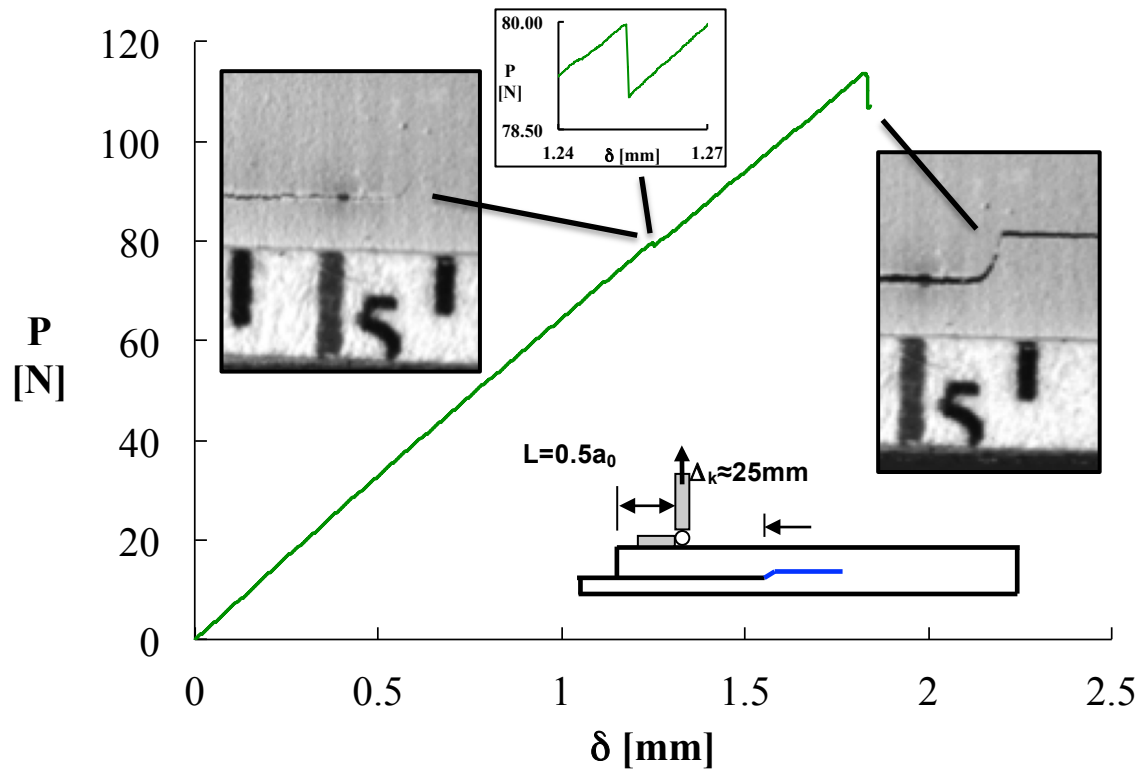
Fig. 7 Load-displacement response and fracture events: L=0.5a_0.
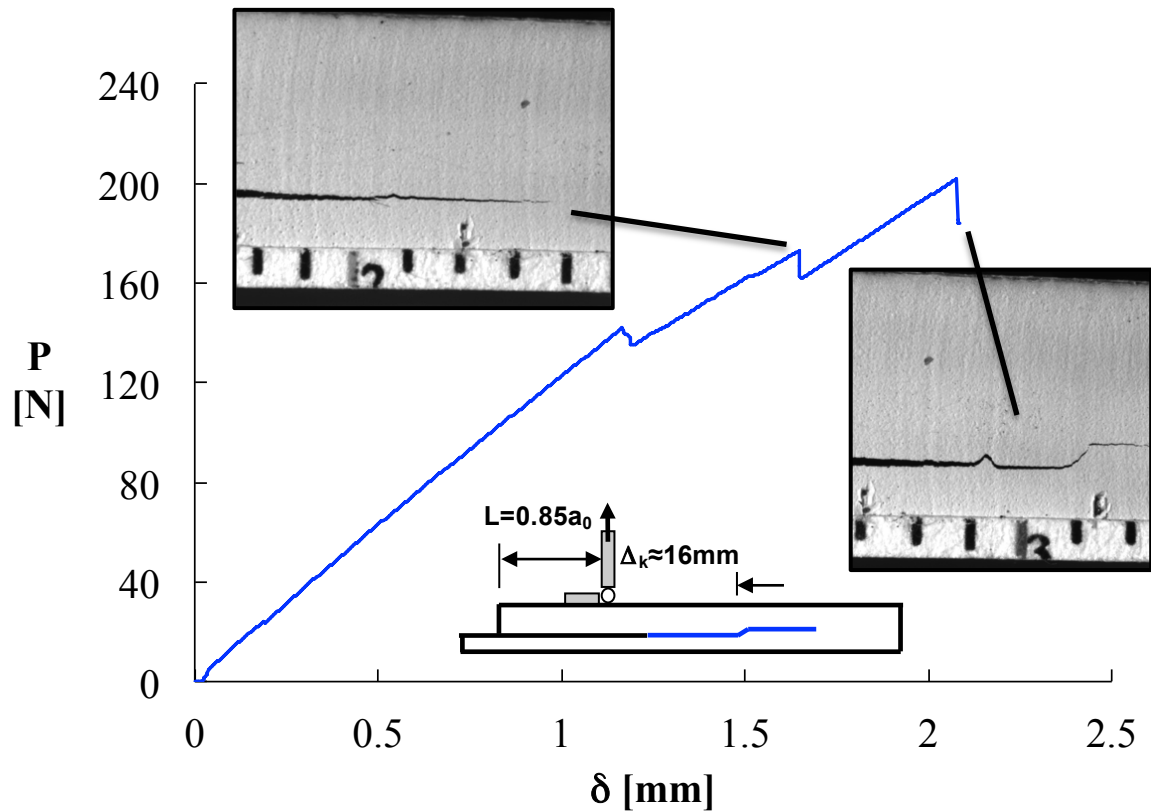
Fig. 8 Load-displacement response and fracture events: L=0.85a_0.
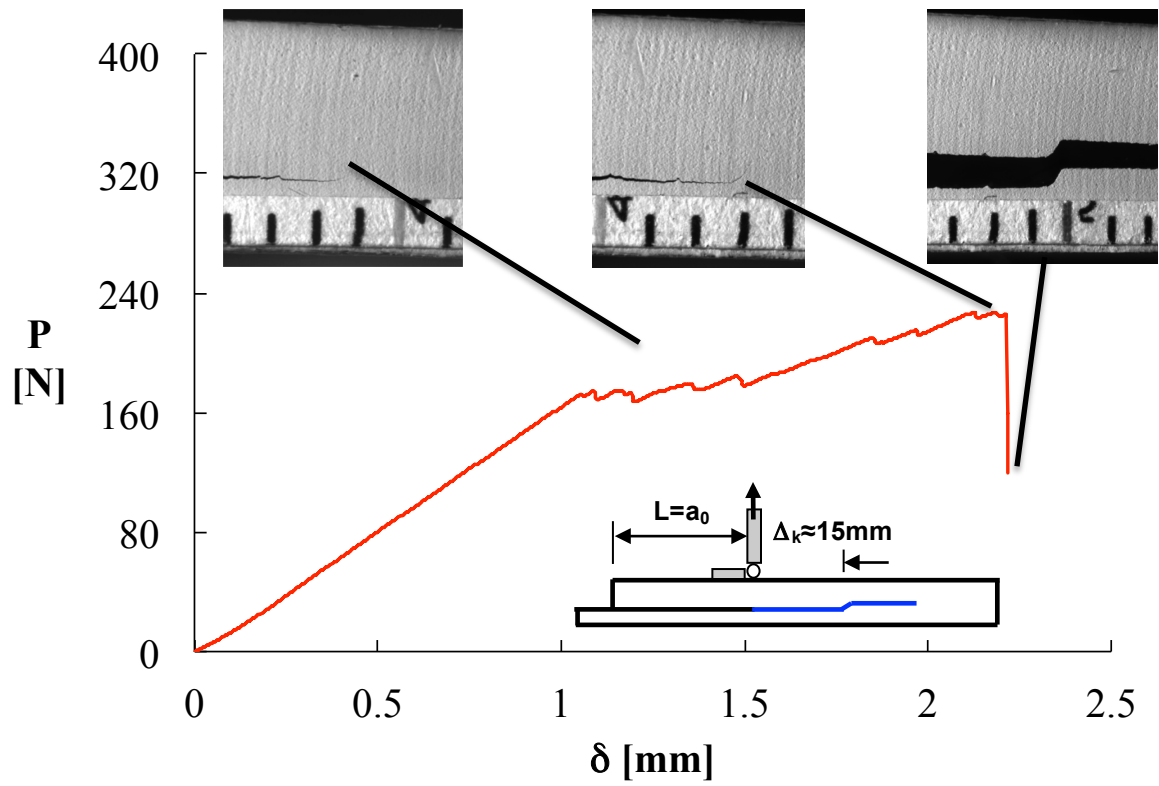
Fig. 9 Load-displacement response and fracture events: L=a₀.
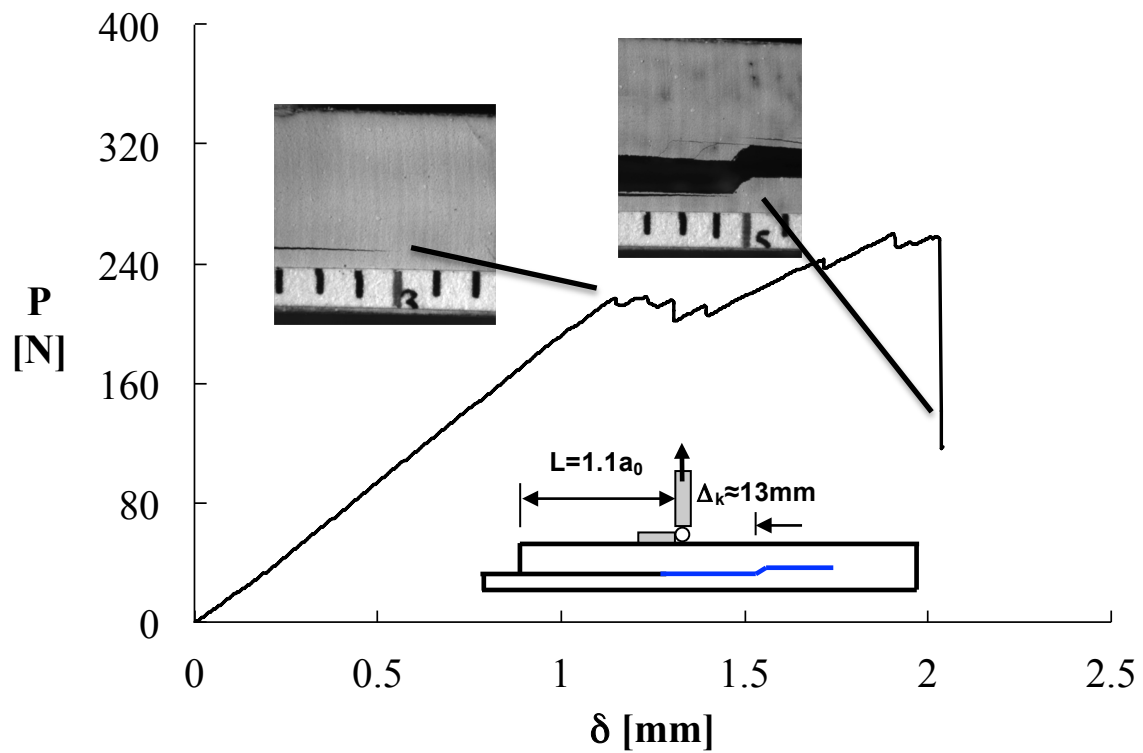
Fig. 10 Load-displacement response and fracture events: L=1.1a₀.
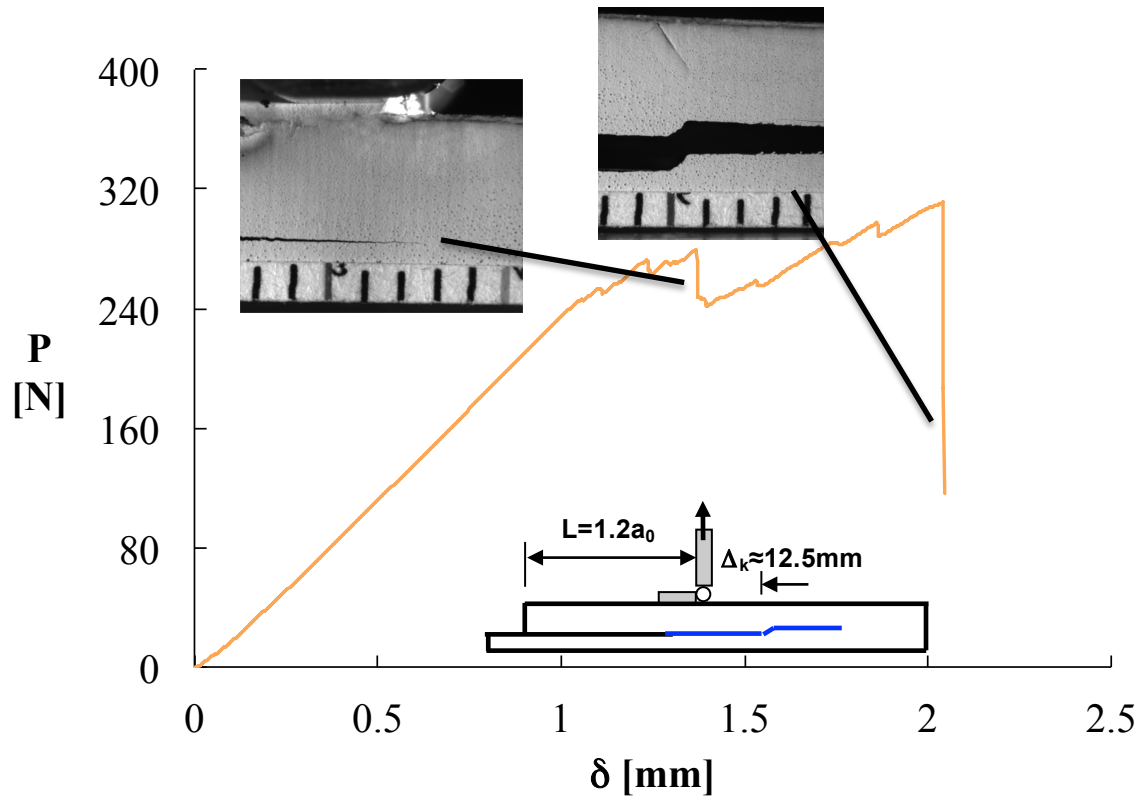
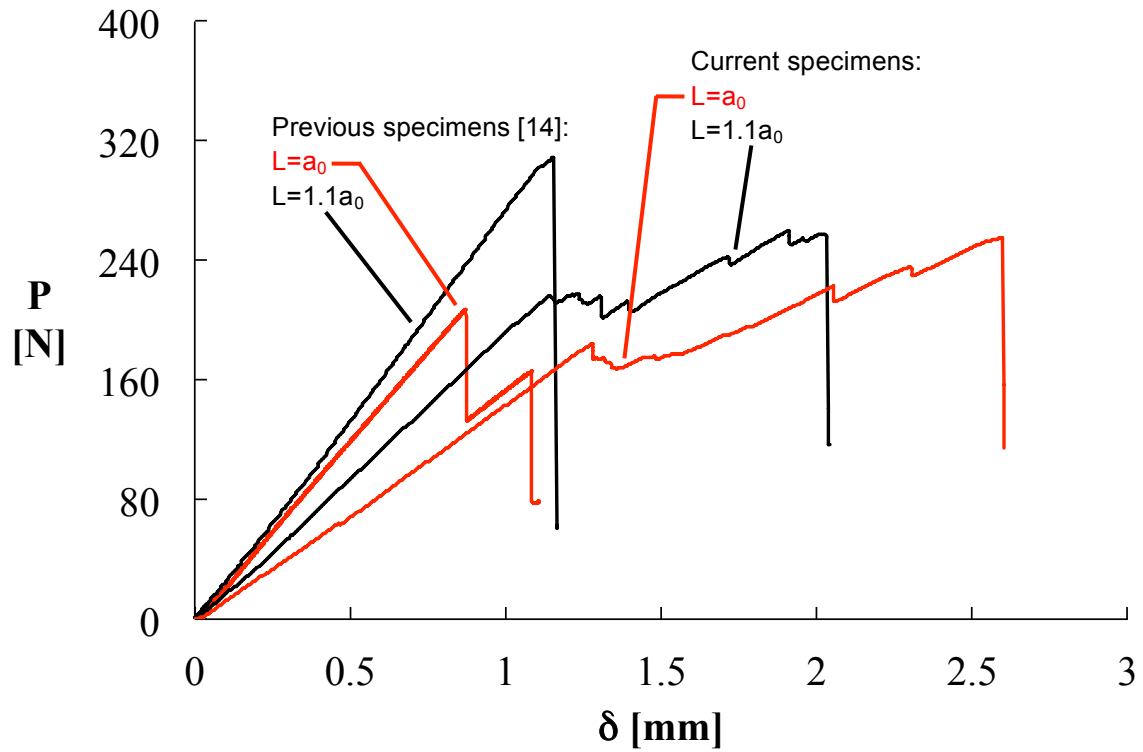Fig. 11 Load-displacement response and fracture events: L=1.2a_0.
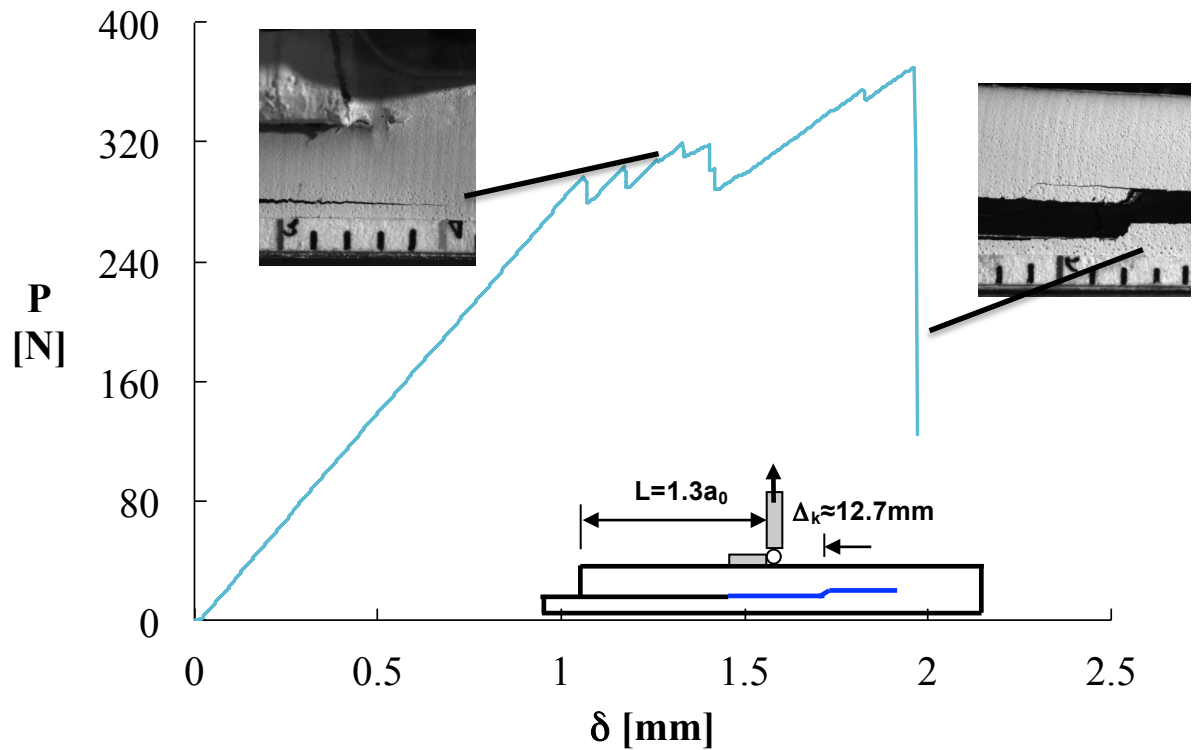
Fig. 12 Load-displacement response and fracture events: L=1.3a_0.

Fig. 13. Load displacement response of current and original specimens (L=a_0 and 1.1a_0).
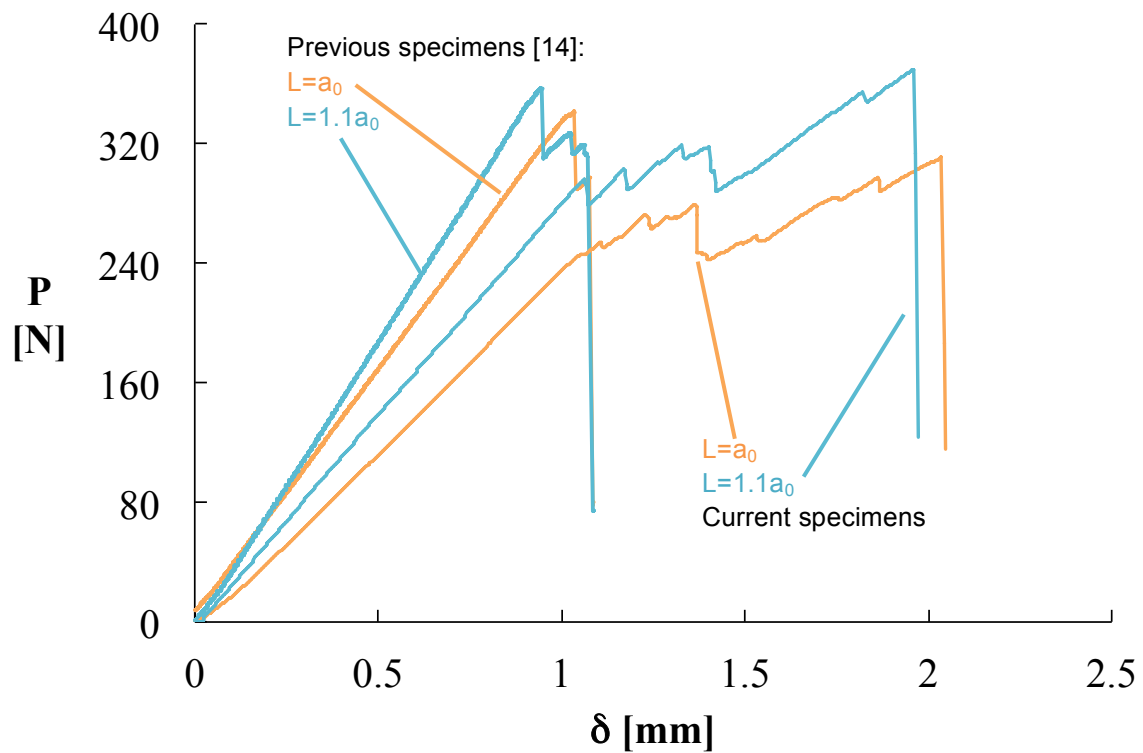
Fig. 14. Load displacement response of current and original specimens (L=1.2a_0 and 1.3a_0).

16
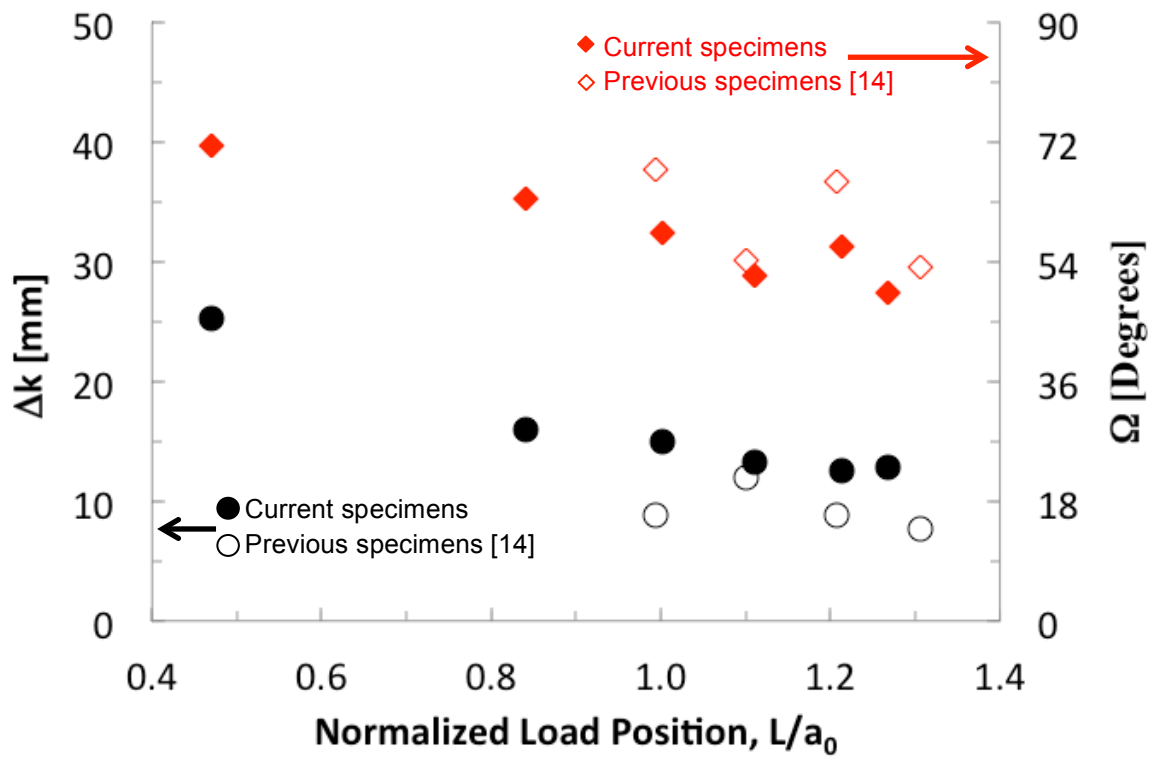
Fig. 15. Effect of load position on migration position and kink angle.
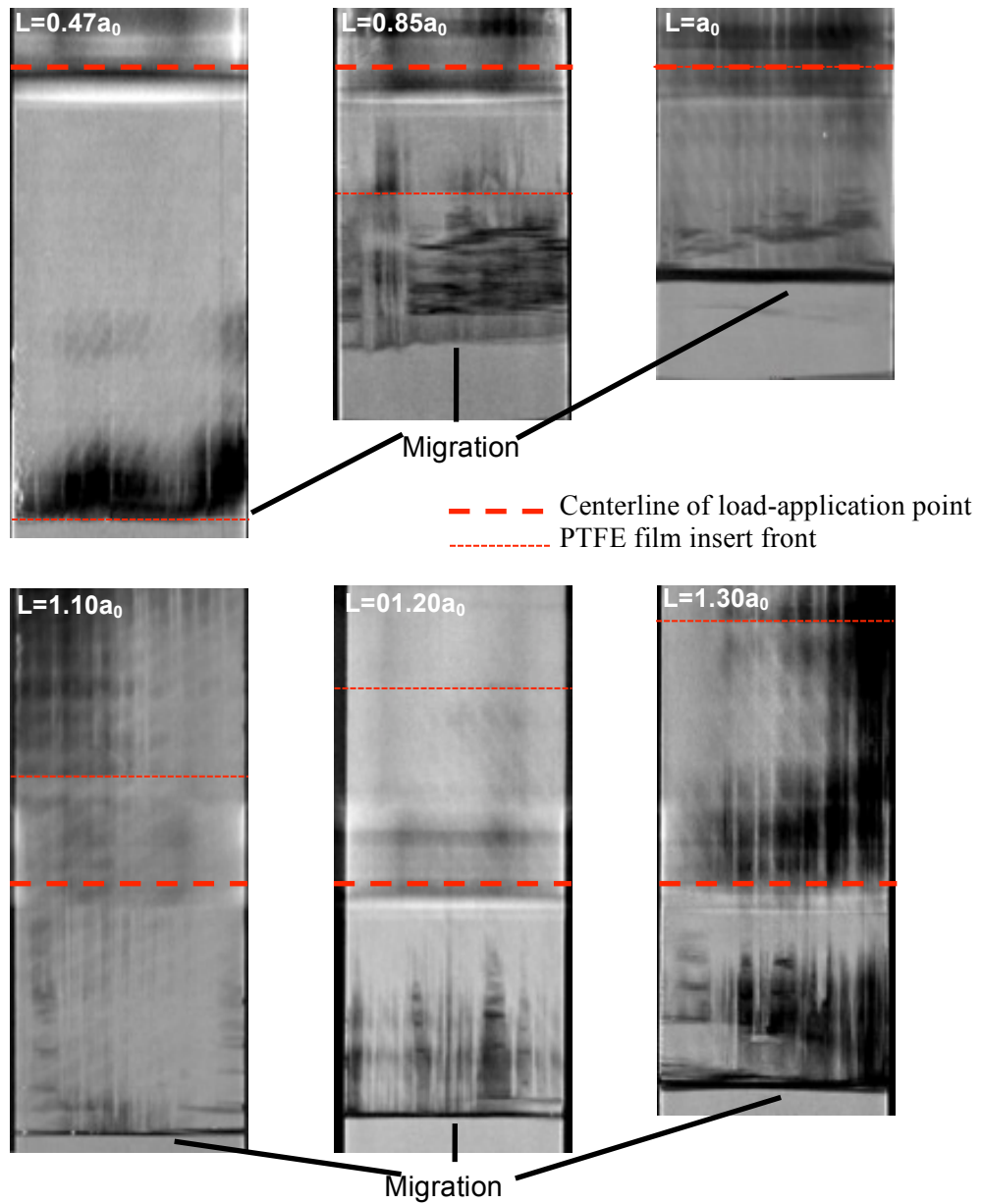
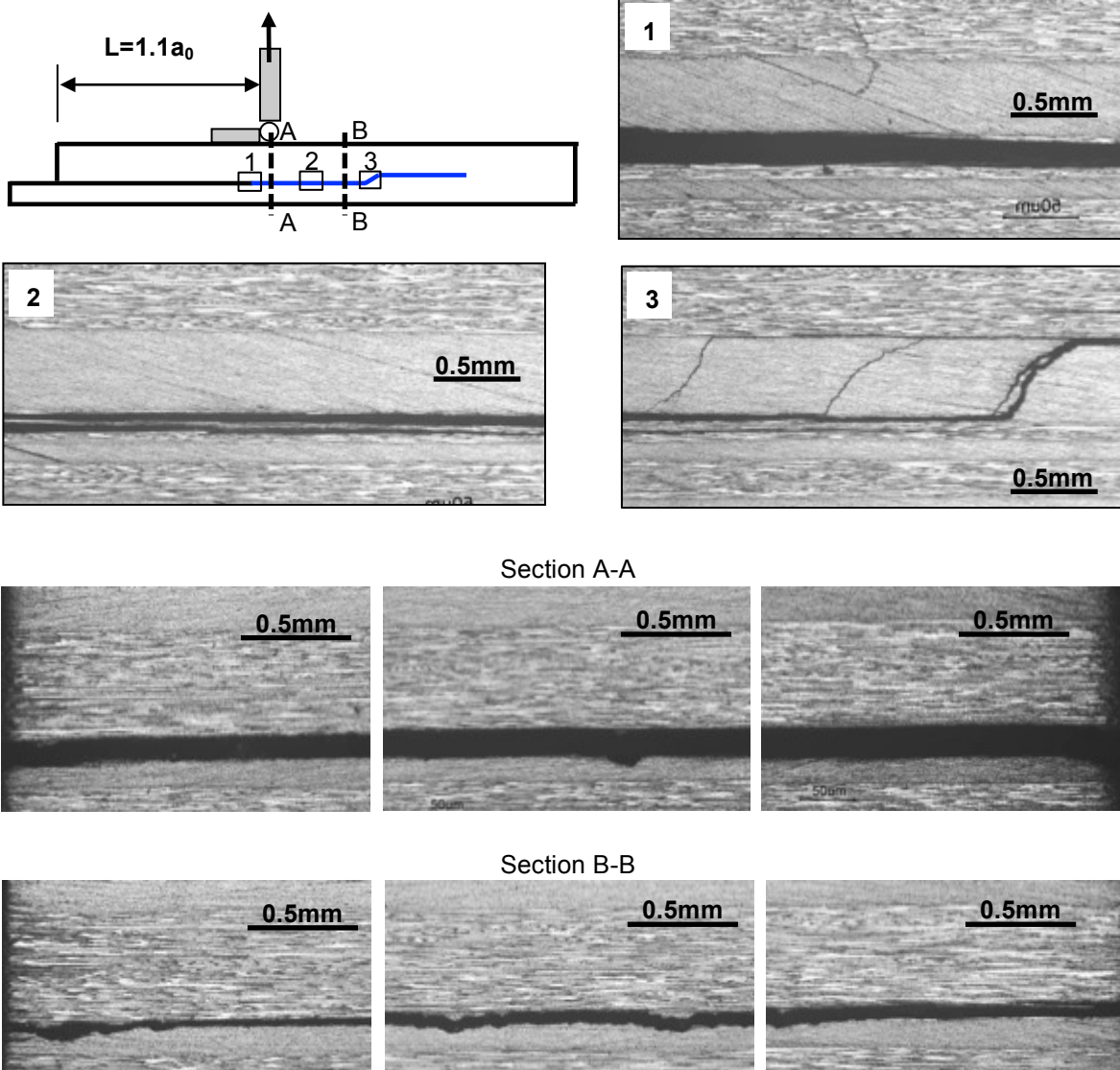Fig. 16. X-ray computed tomography images of upper delamination surface.

Fig. 17. Optical images of section cuts from specimen with $L=1.1a_0$.

REPORT DOCUMENTATION PAGE

Form Approved
OMB No. 0704-0188

1. REPORT DATE *(DD-MM-YYYY)*	2. REPORT TYPE	3. DATES COVERED *(From - To)*
01-07-2014	Technical Memorandum	

4. TITLE AND SUBTITLE

Investigating Delamination Migration in Composite Tape Laminates

5a. CONTRACT NUMBER

5b. GRANT NUMBER

5c. PROGRAM ELEMENT NUMBER

6. AUTHOR(S)

Ratcliffe, James G.; De Carvalho, Nelson V.

5d. PROJECT NUMBER

5e. TASK NUMBER

5f. WORK UNIT NUMBER

794072.02.07.03.03

7. PERFORMING ORGANIZATION NAME(S) AND ADDRESS(ES)

NASA Langley Research Center
Hampton, VA 23681-2199

8. PERFORMING ORGANIZATION REPORT NUMBER

L-20432

9. SPONSORING/MONITORING AGENCY NAME(S) AND ADDRESS(ES)

National Aeronautics and Space Administration
Washington, DC 20546-0001

10. SPONSOR/MONITOR'S ACRONYM(S)

NASA

11. SPONSOR/MONITOR'S REPORT NUMBER(S)

NASA/TM-2014-218289

12. DISTRIBUTION/AVAILABILITY STATEMENT

Unclassified - Unlimited
Subject Category 24
Availability: NASA CASI (443) 757-5802

13. SUPPLEMENTARY NOTES

14. ABSTRACT

A modification to a recently developed test specimen designed to investigate migration of a delamination between neighboring ply interfaces in tape laminates is presented. The specimen is a cross-ply laminated beam consisting of 40 plies with a polytetrafluoroethylene insert spanning part way along its length. The insert is located between a lower 0-degree ply (specimen length direction) and a stack of four 90-degree plies (specimen width direction). The modification involved a stacking sequence that promotes stable delamination growth prior to migration, and included a relocation of the insert from the specimen midplane to the interface between plies 14 and 15. Specimens were clamped at both ends onto a rigid baseplate and loaded on their upper surface via a piano hinge assembly, resulting in a predominantly flexural loading condition. Tests were conducted with the load-application point positioned at various locations along a specimen's span. This position affected the sequence of damage events during a test.

15. SUBJECT TERMS

Delamination; Method; Migration; Test

16. SECURITY CLASSIFICATION OF:			17. LIMITATION OF ABSTRACT	18. NUMBER OF PAGES	19a. NAME OF RESPONSIBLE PERSON
a. REPORT	b. ABSTRACT	c. THIS PAGE			STI Help Desk (email: help@sti.nasa.gov)
U	U	U	UU	24	19b. TELEPHONE NUMBER *(Include area code)* (443) 757-5802

Standard Form 298 (Rev. 8-98)
Prescribed by ANSI Std. Z39.18